BIOLOGY OF REPRODUCTION **80,** 407–414 (2009)
Published online before print 5 November 2008.
DOI 10.1095/biolreprod.108.072900

Quantification of Pelvic Organ Prolapse in Mice: Vaginal Protease Activity Precedes Increased MOPQ Scores in Fibulin 5 Knockout Mice[1]

Cecilia K. Wieslander,[3] David D. Rahn,[3] Donald D. McIntire,[3] Jesús F. Acevedo,[3] Peter G. Drewes,[3] Hiromi Yanagisawa,[4] and R. Ann Word[2,3]

Departments of Obstetrics and Gynecology[3] and Molecular Biology,[4] University of Texas Southwestern Medical Center, Dallas, Texas

ABSTRACT

Two mouse models of pelvic organ prolapse have been generated recently, both of which have null mutations in genes involved in elastic fiber synthesis and assembly (fibulin 5 and lysyl oxidase-like 1). Interestingly, although these mice exhibit elastinopathies early in life, pelvic organ prolapse does not develop until later in life. In this investigation we developed and validated a tool to quantify the severity of pelvic organ prolapse in mice, and we used this tool prospectively to study the role of fibulin 5, aging, and vaginal proteases in the development of pelvic organ prolapse. The results indicate that >90% of *Fbln5*$^{-/-}$ mice develop prolapse by 6 mo of age, even in the absence of vaginal delivery, and that increased vaginal protease activity precedes the development of prolapse.

elastic fibers, female reproductive tract, matrix degradation, matrix metalloproteases, MMP2, MMP9, pelvic organ prolapse, vagina, zymography

INTRODUCTION

Pelvic organ prolapse is a major health problem for women. It has been estimated that 11% of women will undergo at least one surgical procedure for incontinence or prolapse during their lifetime [1]. Despite its common prevalence, the pathophysiology and natural history of pelvic organ prolapse are poorly understood. Large epidemiologic studies have shown that both parity [2, 3] (especially vaginal parity) [4] and aging [2, 3, 5] are major risk factors for the development of pelvic organ prolapse. It has also been proposed that genetic differences in connective tissue composition may contribute to the development of this disorder [6].

Because pelvic organ prolapse takes years to decades to develop in humans, it is difficult to study this disorder in a prospective manner. Therefore, it would be desirable to study this disease prospectively in an animal model with a short lifespan in which induction times and latency periods are much shorter. Two mouse models of pelvic organ prolapse have recently been generated, both of which have null mutations (–/–) in genes involved in elastic fiber synthesis and assembly (fibulin 5 and lysyl oxidase-like 1) [7, 8]. Interestingly, although these mice exhibit elastinopathies early in life (emphysema, loose skin, and vascular abnormalities due to the lack of elastogenesis during development), pelvic organ prolapse develops later. For example, in *Loxl1* null mice, prolapse does not develop until much later in life unless the animals undergo vaginal delivery [8]. Recent results indicate that that a burst of elastic fiber assembly and cross-linking occurs in the vaginal wall postpartum, and that synthesis and assembly of elastic fibers are crucial for recovery of pelvic organ support after vaginal delivery [7]. Based on the relationship between failed elastic fiber synthesis and pelvic organ prolapse, we suggested that changes in elastic fiber degradation occur in the vaginal wall after parturition, thereby leading to failure of pelvic organ support in animals with the inability to synthesize new elastic fibers. Thus, in this investigation we sought to develop a reliable tool to quantify the severity of pelvic organ prolapse in mice and to use this tool prospectively to study the role of fibulin 5 and vaginal proteases in the development of pelvic organ prolapse in a cohort of *Fbln5*$^{-/-}$ and heterozygous (+/–) mice as a function of age.

To study the progression of pelvic organ prolapse objectively in an animal model, it is important to use a quantification system that is accurate and reproducible. Such staging systems have been described in larger animal models, such as the squirrel monkey and the baboon [9, 10]. To our knowledge, there have been no descriptions of staging systems for pelvic organ prolapse in the mouse. In this investigation we developed and validated a scoring system for pelvic organ support in mice and used this system to study the effect of age on pelvic organ prolapse in *Fbln5*$^{-/-}$ mice. To exclude the confounding effects of parity, only nulliparous mice were included. Further, we tested the hypothesis that tissue remodeling of the vaginal wall during pelvic organ prolapse involves activation of matrix metalloproteases (MMPs) that exhibit elastolytic activity. We determined the expression of two MMPs with elastase activity (MMP2 and MMP9) in the vaginal wall of wild-type (WT) and *Fbln5*$^{-/-}$ mice. The results indicate that tissue remodeling of the vaginal wall precedes the development of prolapse in *Fbln5*$^{-/-}$ mice, which develop prolapse as a function of age.

MATERIALS AND METHODS

Study Population

Animals were housed under a 12L:12D light cycle (lights on, 0600–1800 h) at 22°C. Wild-type mice were derived by mating WT males and females. Heterozygous and knockout mice were generated by mating heterozygous females (+/–) with *Fbln5*$^{-/-}$ males, and *Fbln5*$^{-/-}$ females with either *Fbln5*$^{-/-}$ or *Fbln5*$^{+/-}$ males. All studies were conducted in accordance with the standards of humane animal care described in the National Institutes of Health's Guide for the Care and Use of Laboratory Animals and using protocols approved by an institutional animal care and research advisory committee.

[1]Supported by National Institutes of Health grant AG 028048.
[2]Correspondence: R. Ann Word, Division of Urogynecology and Reconstructive Surgery, Department of Obstetrics and Gynecology, University of Texas Southwestern Medical Center at Dallas, 5323 Harry Hines Blvd., Dallas, TX 75390-9032. FAX: 214 648 9242; e-mail: ruth.word@utsouthwestern.edu

Received: 19 August 2008.
First decision: 20 September 2008.
Accepted: 17 October 2008.

eISSN: 1259-7268 http://www.biolreprod.org
ISSN: 0006-3363

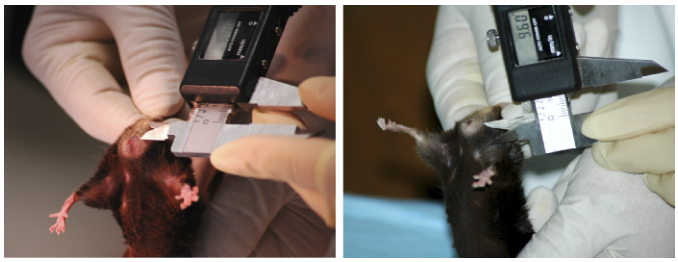

FIG. 1. MOPQ measurements in mice. Perineal body length is measured from the posterior fourchette to the midanus (left). Size of the perineal bulge is determined by measuring from the point of insertion of inner thigh to maximal edge of perineum (right).

Mouse Pelvic Organ Prolapse Quantification Scoring

One investigator held the animal by the scruff of the neck, which resulted in a prolonged, reflex valsalva (evidenced by defecation), while the other investigator performed the measurements using a caliper with the precision of one hundredth of a millimeter (Fig. 1). Six assessments were performed in each animal: 1) grade of perineal bulge, 2) height of perineal bulge, 3) cervical descent, 4) anal prolapsed, 5) perineal body length, and 6) vaginal diameter (Table 1). Perineal bulge, cervical descent, and anal prolapse were measured on ordinal scales (0–4, 0–3, and 0–2, respectively; Table 1). The height of the perineal bulge was measured in millimeters from the point of insertion of inner thigh to the maximal edge of perineum (90 degrees to the insertion of the thigh, just posterior to the genital tubercle). The perineal body was measured in millimeters from the posterior fourchette to the midanus. The vaginal diameter was measured in millimeters from the anterior to the posterior vaginal walls at the level of the introitus.

Mouse Pelvic Organ Prolapse Quantification Interobserver and Intraobserver Reliability

Two examiners (C.K.W. and J.F.A.) conducted mouse pelvic organ prolapse quantification (MOPQ) scoring on 19 heterozygotes (+/–) and 30 *Fbln5*$^{-/-}$ female mice. Measurements were taken by the examiner blinded to genotype. Genotype identification was performed separately by the characteristic phenotypic features of *Fbln5*$^{-/-}$ mice (loose skin, short nose, and large cheeks) and the presence (–/–) or absence (–/+) of arterial tortuosity at the time of killing.

Evaluation of the Development of Pelvic Organ Prolapse in Fbln5$^{-/-}$ and Fbln5$^{+/-}$ Mice as a Function of Age

Two examiners (C.K.W. and J.F.A.) conducted MOPQ scoring of *Fbln5*$^{-/-}$ and *Fbln5*$^{+/-}$ mice from November 2005 to July 2006. During this period, two groups of mice were studied. In the first group, single measurements were performed on 15 *Fbln5*$^{-/-}$, 16 *Fbln5*$^{+/-}$, and 15 WT mice of various ages in two established colonies. Of the 15 WT mice, five were young and nulliparous (4 wk), four were older and nulliparous (5 mo), and six were older and multiparous (5–6 mo). In the second group of animals, 39 adult mice (20 *Fbln5*$^{-/-}$ and 19 *Fbln5*$^{+/-}$) were evaluated at monthly intervals. Starting in March 2006, weekly MOPQ measurements were conducted on 61 (33 *Fbln5*$^{-/-}$ and 26 *Fbln5*$^{+/-}$) mice beginning at 3–4 wk of age (immediately after weaning). To determine interobserver reliability, MOPQ scores were conducted by two different investigators on 2 consecutive days. Intraobserver reliability was determined by comparing MOPQ scores from the same observer on 2 consecutive days. The MOPQ scores in nulliparous *Fbln5*$^{-/-}$ and nulliparous heterozygotes were compared. This was an open cohort study. New animals were added to the study when they were weaned from their mother, and animals were removed from the study when they died or were killed. All animals were mated, and if pregnancy occurred they were not included in the analysis.

TABLE 1. The MOPQ system.

Parameter	Measurement
Grade of perineal bulge	
	0 = None
	1 = Detectable but small
	2 = Moderate size bulge
	3 = Huge
	4 = Vagina coming out
Cervical descent	
	0 = Not visible
	1 = Visible on straining inside the introitus
	2 = At the level of the introitus
	3 = Outside the introitus
Anal prolapse	
	0 = None
	1 = Present but mild
	2 = Severe
Height of perineal bulge	mm
Perineal body length	mm
Vaginal diameter	mm

Tissue Processing

After killing, the pubic symphysis was disarticulated. The uterine horns, together with the bladder, cervix, and vagina, were dissected down to the perineal skin. Using microinstruments and a dissection microscope, the uterine horns were removed at the level of the cervicovaginal junction. Perineal skin was removed, and the bladder and urethra were dissected from the anterior vaginal wall. Thereafter, the cervix was removed. For protease activity measurements, the entire vaginal wall was dissected and incised longitudinally, and the vaginal epithelium was removed by scraping with a scalpel. For RNA analysis, tissues were stored at −20°C in RNA_{Later} (Ambion, Austin, TX). Tissues were frozen in liquid N_2 for analysis of enzyme activity.

Real-Time PCR

Tissues were minced and homogenized in 4 M guanidinium isothiocyanate buffer and were layered over 5.7 M cesium chloride and centrifuged overnight at 237 000 × *g* to extract RNA. Concentration of RNA was measured and purity confirmed by spectroscopy. Reverse transcription reactions were conducted with 2 μg total RNA in a reaction volume of 20 μl. Each reaction contained 10 mM dithiothreitol, 0.5 mM dinucleotide triphosphates, 0.015 μg/μl random primers, 40 units of RNase inhibitor (10777–019; Invitrogen, Carlsbad, CA), and 200 units of reverse transcriptase (18064–014; Invitrogen). Primer sequences for amplifications were chosen using published cDNA sequences and the Primer Express program (Applied Biosystems, Foster City, CA). Primers for *Mmp2* and *Mmp9* were chosen such that the resulting amplicons would cross an exon junction, thereby eliminating the potential for false-positive signals from genomic DNA contamination [11]. SYBR Green was used for amplicon detection. Gene expression was normalized to expression of the housekeeping gene β2-microglobulin (*B2m*). Positive controls (mouse liver and spleen) were run on each plate as appropriate, and all assays included no-template controls. All primer sets were tested to ensure that efficiency of amplification over a wide range of template concentrations was equivalent to that of *B2m*. Positive and negative tissue controls for each primer set were included in each reaction. Polymerase chain reactions were carried out in the ABI Prism 7000 sequence detection system (Applied Biosystems). The reverse transcription product from 50 ng RNA was used as template, and reaction volumes (30 μl) contained 1× Master Mix (4309155; Applied Biosystems). Primer concentrations were 900 nM. Cycling conditions were: 2 min at 50°C followed by 10 min at 95°C, and then 40 cycles of 15 sec at 95°C and 1 min at 60°C. A preprogrammed dissociation protocol was used after amplification to ensure that all samples exhibited a single amplicon. Levels of mRNA were determined using the ddCt method (Applied Biosystems) and expressed relative to an external calibrator present on each plate.

MMP2 Protease Activity

Tissues used for protease activity determinations and zymography were dissected as described above. The vaginal tube was incised longitudinally, and the vaginal epithelium was scraped with a scalpel. Thereafter, the tissues were snap frozen in liquid N_2. To measure enzyme activity, tissues were thawed on ice, minced, and washed in PBS until the supernatant was clear. Tissues then were homogenized in MMP2 assay buffer (EnzoLyte 520 MMP-2 Assay Kit; AnaSpec, San Jose, CA) containing 0.1% Triton X-100 (95× volume:tissue wet weight). Thereafter, the homogenates were centrifuged at 10 000 × *g* for 15 min at 4°C. The supernatant was used for determination of protease activity. Protein concentrations were determined using a BCA protein assay and standard curves of bovine serum albumin in appropriate buffers. ProMMP2 enzyme was activated by incubating the tissue homogenates with 1 mM 4-amino-phenylmercuric acetate (APMA) in MMP2 assay buffer for 15 min at 37°C. Enzyme activity was determined using a fluorescently labeled peptide (FRET peptide) as substrate and a standard curve of purified MMP2 as recommended

by the manufacturer (EnzoLyte 520 MMP-2 Assay Kit). Fluorescence intensity was measured at excitation/emission = 490 nm/520 nm every 5–10 min for 40–60 min. Selective protease activity was inhibited by incubating the samples for 30 min with 12.5 mM ethylenediaminetetraacetic acid (EDTA; matrix metalloproteinase inhibitor), 12.5 nM tissue inhibitors of metalloproteinases (TIMP2), 25 mM iodoacetamide (IAMD; cysteine protease inhibitor), and 2.5 mM phenylmethylsulfonyl fluoride (PMSF; serine elastase inhibitor).

Gelatin Zymography

Because MMP2 enzyme activity assays have significant cross-reactivity with other MMPs, gelatin zymography was used to assess both pro and active forms of MMP9 and MMP2 in vaginal tissues. Samples (5 μg per lane) were applied to gelatin polyacrylamide minigels (10%; Invitrogen) in standard SDS loading buffer containing 0.1% SDS with no β-mercaptoethanol, and the samples were not boiled before loading. The gels were run at room temperature at 125 V. After electrophoresis, the gels were soaked in renaturing buffer (2.7% [v/v] Triton X-100 in distilled water) in a shaker for 30 min with one change after 15 min to remove SDS. Next, the gels were soaked in developing buffer (50 mM Tris, 200 mM NaCl, 10 mM $CaCl_2$, and 0.05% Brij 35, pH 7.5) for 30 min, then overnight in fresh buffer at 37°C and then stained with Coomassie brilliant blue-R 250 in 50% methanol and 10% acetic acid, followed by washing with destain (25% methanol, 7% acetic acid) for 1–2 h as needed to optimize signal/background. Clear zones of lysis against a dark background indicated enzyme activity. Areas of lysis were quantified using a Fuji LAS 3000 image analysis system. Conditions of zymography and analysis were quantitative, because enzyme activity was linear with time of incubation and protein loading, and samples for each experiment were applied to the same gel to account for intergel variation.

Statistical Analysis

Interobserver and intraobserver reliabilities were calculated using the kappa statistic for ordinal variables and the Spearman correlation coefficient (r_s) for continuous variables. Statistical analysis was performed using SigmaStat software (Jandel Scientific, San Rafael, CA). To determine whether assessments of pelvic organ prolapse were significantly different with age, data were analyzed using a random-effects model ANOVA. In all cases, the correlation structure was estimated under no restrictions, and the time effect was assumed linear. The fixed effects were genotype (WT/*Fbln5*$^{+/-}$ or *Fbln5*$^{-/-}$), with time as a random effect. Two-way interactions were estimated, and significance levels were reported. In cases in which the outcome variables were fixed nominal values, the probit model was assumed with the same structure as above. Significance levels lower than 0.05 were considered statistically significant. The analyses were conducted using SAS Version 9.1 (SAS Institute, Cary, NC). For analysis of continuous variables in multiple groups, a one-way ANOVA was conducted, followed by Student-Newman-Keuls pairwise comparisons, with $P < 0.05$ considered significant.

RESULTS

Quantification of Pelvic Organ Prolapse in Mice

To quantify the severity of pelvic organ prolapse in mice, we recorded the grade of perineal bulge by visual exam, the extent of cervical descent, and presence or absence of anal prolapse in animals during maximal valsalva (defecation; Table 1). Perineal body length was measured from the posterior fourchette to the midanus (Fig. 1, left), and the magnitude of perineal bulge was quantified by measuring the distance from the point of insertion of inner thigh to maximal edge of perineum (90 degrees to the insertion of the thigh, just posterior to the clitoris; Fig. 1, right). Grade of bulge and cervical descent are illustrated in Figure 2, in which a dilated vaginal opening with visualization of the cervix distinguishes a grade 3 (Fig. 2D) from a grade 2 (Fig. 2C) bulge. Complete eversion of the vaginal vault (Fig. 2E) is grade 4.

MOPQ Interobserver and Intraobserver Reliability

Interobserver reliability of the grade and magnitude of the perineal bulge was excellent, cervical descent was moderate, and anal prolapse was perfect. Interobserver reliability of perineal body length measurements was also excellent, and that of the vaginal diameter was good (Table 2). Intraobserver reliability of the grade and magnitude of the perineal bulge was also excellent, cervical descent was good, and anal prolapse was perfect. Intraobserver reliability of perineal body length measurements and vaginal diameter determinations was excellent (Table 2).

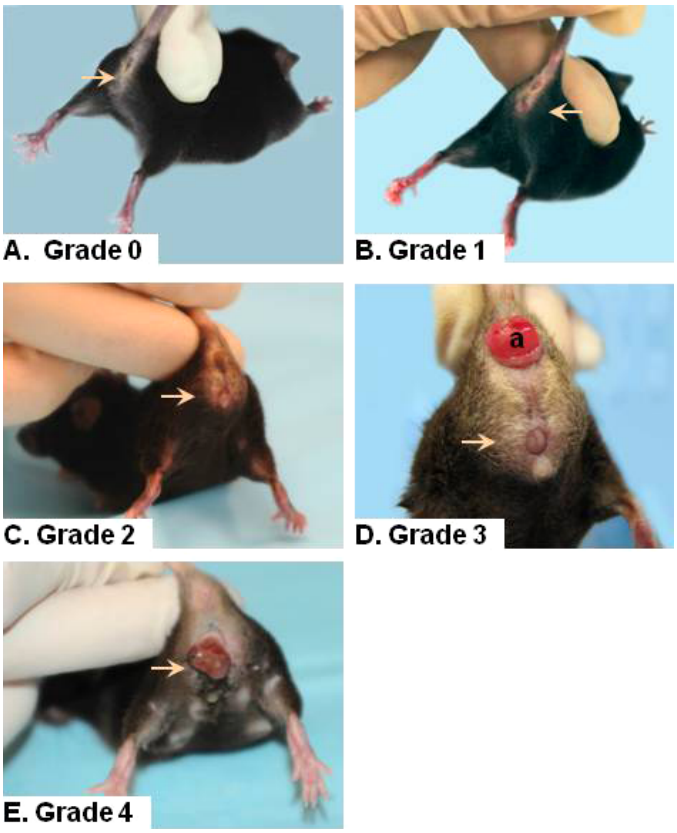

FIG. 2. Stage of prolapse in *Fbln5*$^{-/-}$ mice. Grades 0 (**A**), 1 (**B**), 2 (**C**), 3 (**D**), and 4 (**E**) perineal bulge are assessed by visual inspection. Arrow indicates area of vaginal bulge. Cervical descent is obvious in **D**. a, anal prolapse.

Evaluation of the Development of Pelvic Organ Prolapse in Fbln5$^{-/-}$ and Heterozygote Mice as a Function of Age

Having established the reliability of the MOPQ scoring system, MOPQ assessments were used to determine the effect of age on pelvic organ support in WT, *Fbln5*$^{+/-}$, and *Fbln5*$^{-/-}$ mice. The MOPQ scores were indistinguishable among WT and *Fbln5*$^{+/-}$ animals regardless of age (data not shown). Therefore, 15 WT mice were combined with the heterozygous

TABLE 2. Inter- and intraobserver reliability of MOPQ measurements.

MOPQ measurement	Interobserver agreement/ correlation	Intraobserver agreement/ correlation
Grade of perineal bulge (0, 1, 2, 3, 4)	0.82[a]	0.85[a]
Magnitude of bulge (mm)	0.86[b]	0.88[b]
Cervical descent (0, 1, 2, 3)	0.50[a]	0.71[a]
Anal prolapse (0, 1, 2)	1.0[a]	1.0[a]
Perineal body length (mm)	0.89[b]	0.98[b]
Vaginal diameter (mm)	0.67[b]	0.93[b]

[a] Determined using the kappa statistic.
[b] Determined using Spearman correlation coefficient.

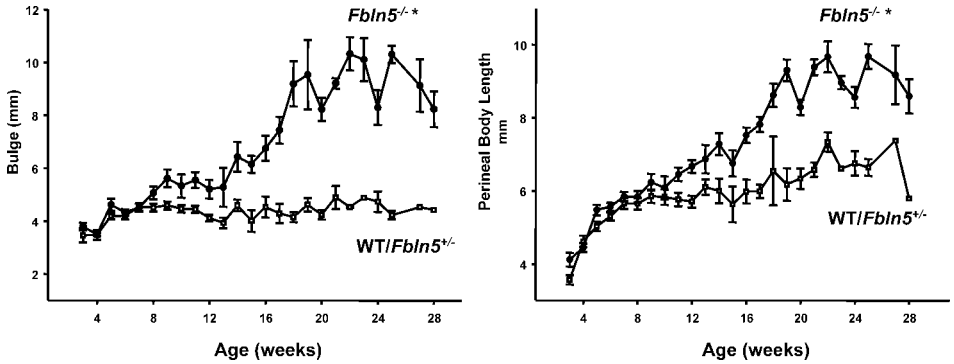

FIG. 3. Effect of age on pelvic organ prolapse in mice. Measurements of perineal bulge (left) and perineal body length (right) are plotted as a function of age in WT/*Fbln5*$^{+/-}$ (open squares) or *Fbln5*$^{-/-}$ (solid circles) mice. Data represent mean ± SEM of 33 *Fbln5*$^{-/-}$ and 41 WT/*Fbln5*$^{+/-}$ mice. *$P \leq 0.05$ compared with WT/*Fbln5*$^{+/-}$.

group to increase the power of the study. The magnitude of perineal bulge and length of the perineal body increased significantly with age in *Fbln5*$^{-/-}$ mice but not in WT/*Fbln5*$^{+/-}$ animals (Fig. 3). In *Fbln5*$^{-/-}$ mice, differences in size of the perineal bulge were observed as early as 8–9 wk of age, whereas small but statistically significant increases in perineal body length were observed at 10–12 wk (Fig. 3). Perineal body length increased in both WT/*Fbln5*$^{+/-}$ and *Fbln5*$^{-/-}$ animals from 3 to 8 wk of age because of growth and increase in body size. Thereafter, subtle differences in perineal body length occurred in WT/*Fbln5*$^{+/-}$ animals with aging. Perineal body length was 5.8 ± 0.09 in WT/*Fbln5*$^{+/-}$ animals from 10–16 wk of age and 6.6 ± 0.14 mm after 20 wk of age ($P \leq 0.01$). This subtle change in perineal body length may be due to increased weight gain during this time period rather than laxity of perineal support. Perineal bulge measurements did not increase in WT/*Fbln5*$^{+/-}$ mice.

To examine the effect of age on MOPQ variables (bulge grade, cervical descent, and vaginal diameter), data from *Fbln5*$^{-/-}$ and WT/*Fbln5*$^{+/-}$ mice were incorporated in a statistical model to study the interaction between the variable and genotype or age (Fig. 4). (In this model, progression of prolapse was assumed to be linear, and therefore predicted bulge grade 4 and large increases in vaginal diameter, although these variables did not increase after 6 mo of age.) Nevertheless, significant differences in bulge grade, cervical descent, magnitude of perineal bulge, perineal body length, and vaginal diameter occurred in *Fbln5*$^{-/-}$ mice with increasing age, but no changes in these parameters were observed in WT/*Fbln5*$^{+/-}$ mice. Although none of the WT/*Fbln5*$^{+/-}$ animals developed anal prolapse, the number of *Fbln5*$^{-/-}$ mice with anal prolapse was too small for meaningful statistical comparisons (n = 4 of 74 animals with prolapse).

Regulation of Elastolytic MMPs in Vaginal Tissues from Fbln5$^{-/-}$ *Mice*

To investigate a potential role for MMP2 and MMP9 in the vaginal wall of *Fbln5*$^{-/-}$ mice, expression of these enzymes was determined by gelatin zymography and compared with that of WT mice. ProMMP9 (92 kDa) was highly expressed in the vaginal wall of *Fbln5*$^{-/-}$ animals, although expression of the enzyme was low in WT animals (Fig. 5). Both MMP9 and MMP2 were increased significantly in vaginal tissues from *Fbln5*$^{-/-}$ mice. APMA resulted in conversion of proMMP9 to the active 86-kDa MMP9 and conversion of proMMP2 (72 kDa) to 68- and 65-kDa active enzymes. Interestingly, after APMA treatment both 68- and 65-kDa forms of active MMP2 were increased significantly in vaginal tissues from *Fbln5*$^{-/-}$ mice (Fig. 5). Active and total MMP2 enzyme activities were further quantified using a fluorescently labeled peptide (FRET peptide) as substrate and a standard curve of purified MMP2 with or without APMA (Fig. 5C), confirming significantly increased MMP2 activity in tissues from *Fbln5*$^{-/-}$ animals. As observed previously [11], APMA resulted in paradoxical decreases in MMP2 activity in vaginal homogenates from WT animals. In contrast, cleavage of proMMP2 with APMA in vaginal homogenates from *Fbln5*$^{-/-}$ was increased (Fig. 5C), suggesting that APMA-cleaved activity in these vaginal tissues is increased (or more stable) than that in nonpregnant WT animals.

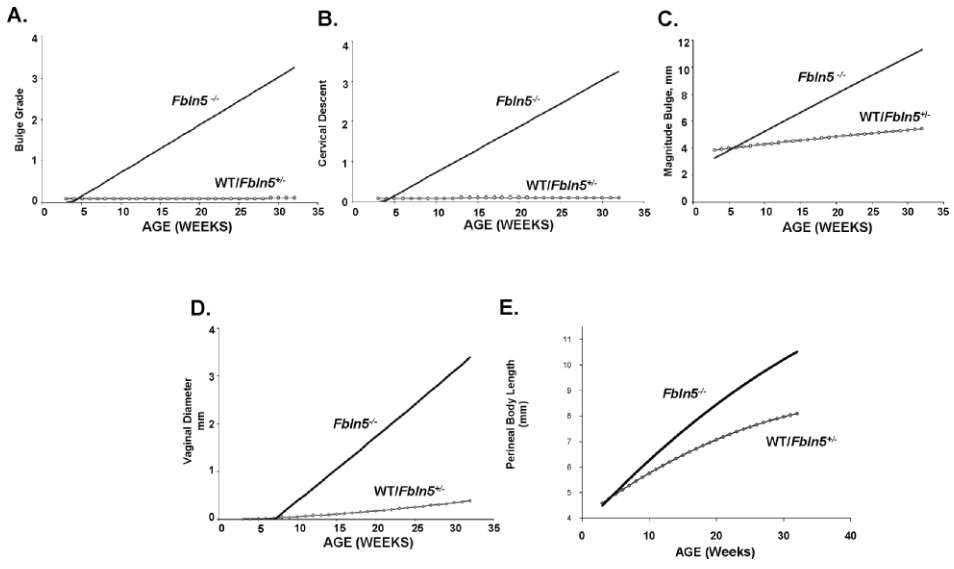

FIG. 4. Random-effects model of the effect of age on MOPQ measurements in *Fbln5*$^{-/-}$ mice. Nominal data from mice at various ages were incorporated in a random-effects model. Perineal bulge grade (**A**), cervical descent (**B**), magnitude of bulge (**C**), vaginal diameter (**D**), and perineal body length (**E**) were found to be significantly different as a function of age in *Fbln5*$^{-/-}$ (solid lines), but not WT/*Fbln5*$^{+/-}$ (dashed lines). The model significantly predicts experimental results and demonstrates significant differences among WT/*Fbln5*$^{+/-}$ and *Fbln5*$^{-/-}$ animals.

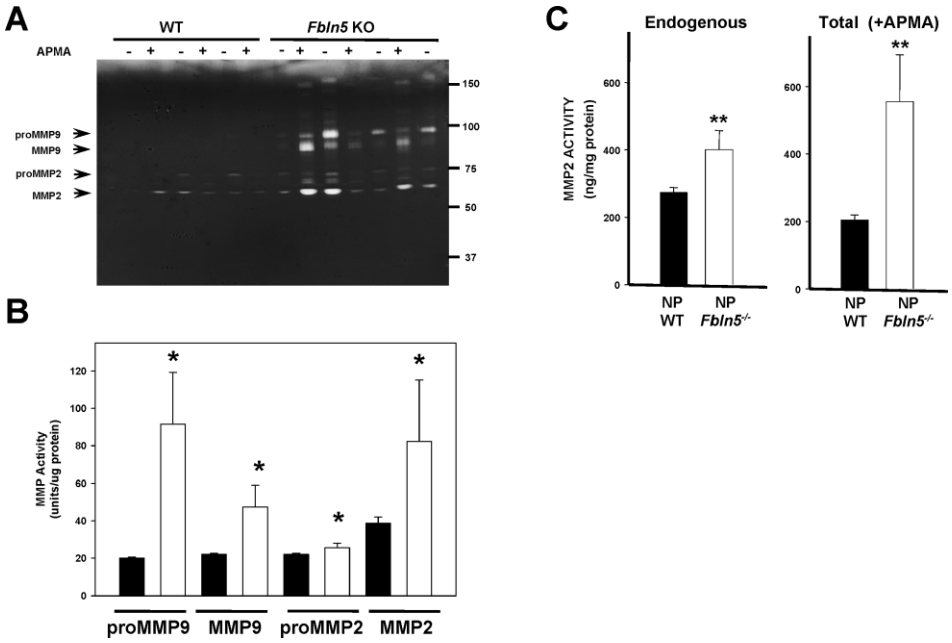

FIG. 5. MMP2 and MMP9 enzyme activities in WT and *Fbln5*$^{-/-}$ mice. Tissue extracts were incubated with and without APMA to determine pro and active forms of MMP2 and MMP9. **A**) Representative gelatin zymogram of pro and active MMP9 and MMP2 in the presence or absence of APMA in vaginal tissue extracts from WT and *Fbln5*$^{-/-}$ (*Fbln5* KO) mice. **B**) Densitometry of endogenous MMP activity using zymography of tissue extracts from WT (solid bars) and *Fbln5*$^{-/-}$ (open bars) mice. Data represent mean ± SEM of five animals in each group. *$P < 0.05$ compared with WT. ug, microgram. **C**) MMP2 enzyme activity was determined using a fluorescent substrate as described in *Materials and Methods*. In WT animals, total MMP2 activity (+APMA) was less than that of active enzyme, possibly because of binding of endogenous inhibitors to APMA-cleaved enzyme. Total (+APMA) and active (−APMA, labeled Endogenous) enzyme activities were increased in vaginal tissues from *Fbln5*$^{-/-}$ animals. **$P \leq 0.01$ compared with corresponding activity in vaginal tissues from WT mice. NP, nonpregnant.

Endogenous MMP2 activity was characterized further in tissue homogenates from *Fbln5*$^{-/-}$ mice (Fig. 6). EDTA resulted in inhibition of enzyme activity in vaginal tissues from both WT and *Fbln5*$^{-/-}$ nonpregnant animals (Fig. 6). TIMP2 also inhibited enzyme activity to a similar extent in both WT and *Fbln5*$^{-/-}$ animals. In contrast, MMP2 enzyme activity in vaginal tissues from *Fbln5*$^{-/-}$ mice was less sensitive to IAMD (an inhibitor of cysteine proteases) and PMSF (an inhibitor of serine proteases; Fig. 6).

MMP2 and MMP9 are regulated at both transcriptional and posttranslational levels. Both contain an N-terminal propeptide domain, a catalytic domain, and a hemopexinlike C-terminal domain. They are secreted as inactive proforms called zymogens, and they undergo proteolytic cleavage to become active enzymes. To determine whether *Mmp9* or *Mmp2* mRNA levels were altered in *Fbln5*$^{-/-}$ mice, RNA was isolated from vaginal muscularis obtained from nonpregnant virginal cycling mice and *Fbln5*$^{-/-}$ mice (Fig. 7). Interestingly, mRNA levels of *Mmp2* and *Mmp9* were not increased in vaginal tissues from *Fbln5*$^{-/-}$ mice, suggesting that the regulation of enzyme activity occurs at the posttranscriptional level.

Expression of MMP2 and MMP9 in Vaginal Tissues from Young Fbln5$^{-/-}$ *Mice*

To determine whether increases in MMP activity preceded prolapse of the vaginal wall, vaginal tissues were obtained from *Fbln5*$^{-/-}$, *Fbln5*$^{+/-}$, and WT mice at 4 wk of age (i.e., >6 wk before development of prolapse), and MMP2 and MMP9 activities were determined using gelatin zymography. Compared with WT, proMMP9 was increased 3.6-fold in vaginal tissues from young *Fbln5*$^{-/-}$ mice before prolapse and 1.8-fold in *Fbln5*$^{+/-}$ ($P < 0.001$; Fig. 8). Similarly, active MMP9 was increased 3-fold, compared with 1.6-fold in heterozygotes ($P < 0.001$). These values are comparable to upregulation of MMP9 in *Fbln5*$^{-/-}$ mice with prolapse (Fig. 5). The magnitude of increase in MMP2 in the vaginal wall of *Fbln5*$^{-/-}$ animals without prolapse was less than that of MMP9 (Fig. 8). Thus, small increases in MMP2 and larger increases in MMP9 in the vaginal wall preceded the development of prolapse in *Fbln5*$^{-/-}$ mice. Further, *Fbln5*$^{+/-}$ animals appear to have an intermediate degree of increased MMP9 activity in the vagina, but no evidence of prolapse and normal elastic fiber morphology (data not shown).

DISCUSSION

In this investigation we found that the MOPQ is a reliable tool for quantifying the severity and progression of pelvic organ prolapse in mice. Measurements of cervical descent and vaginal diameter were less reliable than assessments of the magnitude of perineal bulge and perineal body length. It is likely that differences in assessment of vaginal diameter were due to the effect of the estrus cycle on this measurement.

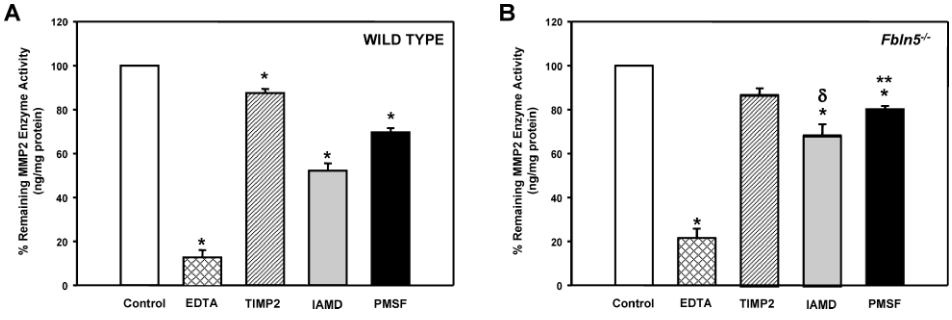

FIG. 6. Enzyme inhibitor profile of MMP2 in vaginal tissues from WT and *Fbln5*$^{-/-}$ mice. Protein extracts of vaginal tissues from WT (**A**) and *Fbln5*$^{-/-}$ (**B**) mice were incubated with vehicle (Control), EDTA (12.5 mM), TIMP2 (12.5 mM), IAMD (25 mM), or PMSF (22.5 mM) for 30 min prior to quantification of MMP2 enzyme activity. Each bar represents mean ± SEM of four tissues in each group, except for IAMD (n = 3). *$P \leq 0.05$ compared with control tissues; **$P \leq 0.01$ compared with WT values, $^{\delta}P = 0.056$ compared with WT values.

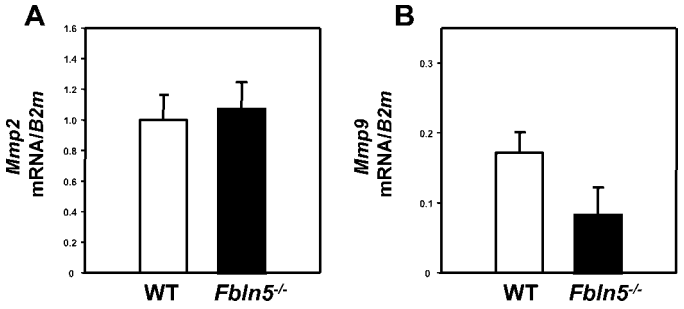

FIG. 7. Expression of *Mmp2* and *Mmp9* mRNA in vaginal tissues from WT and *Fbln5*$^{-/-}$ mice. Real-time PCR was used to determine the relative abundance of *Mmp2* (**A**) and *Mmp9* (**B**) mRNA in vaginal tissues from WT (open bars) and *Fbln5*$^{-/-}$ (solid bars) nonpregnant mice. All knockout animals exhibited pronounced pelvic organ prolapse. *Mmp* mRNA was expressed relative to that of β2-microglobulin (*B2m*) and normalized to that of positive controls, which served as external standard (mouse liver for *Mmp2*, and mouse spleen for *Mmp9*). Data represent mean ± SEM of five to seven mice in each group.

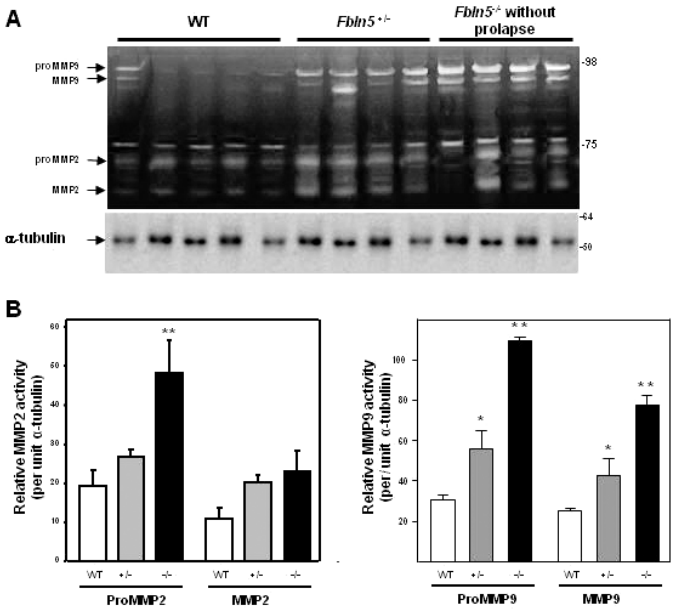

FIG. 8. Vaginal protease activity in *Fbln5*$^{-/-}$ mice before pelvic organ prolapse. **A**) Gelatin zymogram illustrating gelatinase activities of MMP2 and MMP9 in vaginal tissues from 4-wk-old *Fbln5*$^{-/-}$ mice (i.e., before the age of prolapse onset) with age-matched virginal *Fbln5*$^{+/-}$ and WT controls. Immunoblot for alpha tubulin beneath the zymogram demonstrates even protein loading. Data represent areas of gel lysis in density units normalized to density units of alpha tubulin. **B**) Densitometric quantification of MMP2 and MMP9 activity in the vaginal wall of young WT, *Fbln5*$^{+/-}$, and *Fbln5*$^{-/-}$ mice. Data represent mean ± SEM of four to five tissues from each genotype. $^{*}P \leq 0.05$ compared with WT; $^{**}P \leq 0.05$ compared with *Fbln5*$^{+/-}$ or WT.

Vaginal opening is also an indicator of sexual maturity in rodents [12] and an indicator of sexual receptivity during the estrus cycle [13–15]. Therefore, vaginal diameter measurements were likely to be influenced by cycle stage and hormonal milieu. Because cervical descent was more likely to be visualized during vaginal opening, this assessment was also likely to be influenced by the estrus cycle. It is also possible that cervical descent and vaginal diameter were more sensitive to change in valsalva effort among mice or to the degree of bladder distention. Nevertheless, both measurements correlated with the severity of prolapse in *Fbln5*$^{-/-}$ mice. The results demonstrate substantial interexaminer and intraexaminer reproducibility in both the quantification of pelvic organ descent (as indicated by the perineal bulge) and in the ordinal staging of prolapse. The MOPQ is easy to perform and takes less than 1 min to complete. This system may be useful in quantification of prolapse in other mouse models of this disorder.

Other major findings of this study are 1) that progressive deterioration of pelvic organ support occurs in animals deficient in Fbln5, even in the absence of vaginal parity, and 2) that loss of pelvic organ support was preceded by substantial upregulation of vaginal protease activity. Epidemiologic studies suggest that aging and vaginal birth are two of the major risk factors for the development of pelvic organ prolapse. The mechanisms by which aging leads to failure of pelvic organ support are not known. Further, the mechanisms that mediate the delayed manifestations of childbirth-associated injuries of the pelvic floor are not understood. Although denervation or injury to the levator ani is believed to contribute to the development of pelvic organ prolapse in women, a potential role for fibromuscular connective tissue in the pathophysiology of pelvic organ prolapse has been proposed by us [16, 17] and others [18]. Studies conducted with vaginal tissues from women with or without pelvic organ prolapse, however, provide little information regarding the pathogenesis of this disorder. Prolonged stretch, mechanical stress, and hypoxia within the vaginal wall may produce secondary effects that contribute to the progressive deterioration of pelvic organ support, but these factors may be unrelated to its pathogenesis. Recent findings in mice with null mutations in genes encoding lysyl oxidase-like 1 [8] or *Fbln5* [7] indicate that these proteins are crucial for pelvic organ support in mice. Both proteins are involved in synthesis and assembly of elastic fibers. It has been suggested, therefore, that defects in elastic fiber assembly and synthesis may predispose or lead to pelvic organ prolapse in women [7]. Here, we found that although they are born with tortuosity of blood vessels and histologic features of emphysema [19], *Fbln5*$^{-/-}$ mice do not develop pelvic organ prolapse until several weeks after sexual maturity (10–12 wk). Thereafter, the severity of prolapse increases rapidly with age such that by 6 mo of age, >90% of *Fbln5*$^{-/-}$ females have advanced prolapse. The MOPQ measurements on 18 animals ranging from 6 to 9 mo of age indicate that substantial progression of prolapse does not appear to occur after 6 mo of age (data not shown), although the lifespan of *Fbln5*$^{-/-}$ mice is similar to that of WT animals [19].

Matrix degradation and protease activation have been suggested to play a role in the pathophysiology of pelvic organ prolapse [11, 20–26]. Vaginal extracellular matrix undergoes continuous remodeling in response to varying levels of hormones in the estrous cycle [27–31], during pregnancy [31], and in the postpartum time period [11]. Because elastic fiber degradative products have been shown to increase activation of matrix proteases in affected tissues [32–34], we considered the possibility that MMP activity may be increased in animals in which elastic fiber synthesis is abnormal. MMP9 degrades components of the extracellular matrix with high specific activity for denatured collagens, native collagens of types IV, V, and XI, and elastin, but not native type I collagen, proteoglycans, or laminins. MMP9 also cleaves a variety of non-extracellular matrix molecules, such as interleukin 1β, substance P, myelin basic protein, and amyloid β peptide [35]. MMP9 is expressed frequently at sites of active tissue remodeling and neovascularization. During embryonic development it is highly expressed by trophoblast cells and osteoclasts. In adulthood, however, its expression is predominantly limited to inflammatory cells and in pathological

processes, such as inflammatory arthritis, tumor invasion, skin blistering diseases, corneal ulcers, and Alzheimer disease [35]. Mice with null mutations in *Mmp9* exhibit an abnormal pattern of skeletal growth plate vascularization and ossification [36]. Interestingly, deficiency of MMP2 does not appear to result in any significant developmental or physiological impairment [37]. Both MMP9 and MMP2 were upregulated in vaginal tissues of adult *Fbln5*$^{-/-}$ mice, and MMP2 enzyme activity in the *Fbln5*$^{-/-}$ vagina was uniquely regulated and less sensitive to protease inhibitors. Further, results indicate that MMP9 activity was upregulated significantly several weeks prior to the onset of prolapse. Interestingly, MMP9 activity was also upregulated in vaginal tissues from *Fbln5*$^{+/-}$ mice, but prolapse was not observed in these animals. Because elastic fibers are normal in *Fbln5*$^{+/-}$ mice, haploinsufficiency appears to be adequate for elastogenesis but not for suppression of MMP9. Increased MMP9 activity in the presence of normal elastic fibers does not appear to lead to pelvic organ prolapse in mice. Elastic fiber defects alone, however, are probably not sufficient to effect MMP9 activation, because increased gelatinolytic activity was not observed in the aorta or skin from *Fbln5*$^{-/-}$ animals (our unpublished data). Hence, fibulin 5 may suppress protease activity in the vaginal wall, and we believe that this activity is unique in adult tissues that undergo continuous remodeling (such as the vagina). Experiments are ongoing to test these hypotheses. Nevertheless, our results with young *Fbln5*$^{-/-}$ mice suggest that MMP9 may play a pivotal role in development of prolapse in the presence of abnormal elastic fiber synthesis. This finding is especially relevant because proMMP2 [23] and MMP9 [26] have been found to be upregulated in the vaginal wall of women with pelvic organ prolapse.

Although the source of MMP9 in the vaginal wall is unknown, secretion of MMP9 is increased significantly in cultured vaginal stromal cells from *Fbln5*$^{-/-}$ compared with WT mice (our unpublished data). Because MMP2 and MMP9 are known to be produced by smooth muscle cells, the source of MMP9 in the vaginal wall is most likely from vaginal stroma (fibroblasts and smooth muscle cells). Activation of proMMP2 occurs at the cell surface through formation of trimolecular complexes with membrane-type 1-MMP and TIMP2. Activation of MMP9 requires other proteinases, such as MMP2, MMP3, and MMP13, or serine proteinases, such as trypsin and plasmin. To add another layer of complexity, plasminogen activator inhibitor 1 (PAI1), official symbol SERPINE1, may inhibit elastic fiber degradation by suppressing plasmin-induced activation of MMPs [38]. Once initiated, degradation products of elastin and microfibrils further accelerate proteolytic cascades through activation of proinflammatory pathways [32, 39].

In summary, the results of this study suggest that the absence of fibulin 5 in the vaginal wall leads to not only abnormal elastogenesis but also increased protease activity and age-dependent loss of pelvic organ support. The inability to repair or synthesize new elastic fibers because of genetic defects in elastic fiber synthesis and assembly may then lead to failure of matrix regeneration in connective tissues that support the pelvic floor. Lack of fibulin 5 appears to not only play an important structural role in the vaginal wall, but also may play an important role in suppressing protease activation that precedes the development of clinical pelvic organ prolapse in mice.

ACKNOWLEDGMENTS

We wish to thank Ms. Shelby Chapman for expert assistance with management of the animal colony, Mr. Patrick Keller for expert technical assistance, and Dr. Hiromi Yanagisawa for careful reading of the manuscript.

REFERENCES

1. Olsen AL, Smith VJ, Bergstrom JO, Colling JC, Clark AL. Epidemiology of surgically managed pelvic organ prolapse and urinary incontinence. Obstet Gynecol 1997; 89:501–506.
2. Mant J, Painter R, Vessey M. Epidemiology of genital prolapse: observations from the Oxford Family Planning Association Study. Br J Obstet Gynaecol 1997; 104:579–585.
3. Hendrix S, Clark A, Nygaard I, Aragaki A, Barnabei V, McTiernan AA. Pelvic organ prolapse in the women's health initiative: gravity and gravidity. Am J Obstet Gynecol 2002; 186:1160–1166.
4. Luckacz ES, Lawrence JM, Contreras R, Nager CW, Luber KM. Parity, mode of delivery, and pelvic floor disorders. Obstet Gynecol 2006; 107: 1253–1260.
5. Swift S, Woodman P, O'Boyle A, Kahn M, Valley M, Bland D, Wang W, Schaffer J. Pelvic Organ Support Study (POSST): the distribution, clinical definition, and epidemiologic condition of pelvic organ support defects. Ame J Obstet Gynecol 2005; 192:795–806.
6. Norton PA, Baker JE, Sharp HC, Warenski JC. Genitourinary prolapse and joint hypermobility in women. Obstet Gynecol 1995; 85:225–228.
7. Drewes PG, Yanagisawa H, Starcher B, Hornstra IK, Csiszar K, Marinis SI, Keller P, Word RA. Pelvic organ prolapse in Fibulin-5 knockout mice: pregnancy changes in elastic fiber homeostasis in mouse vagina. Am J Pathol 2007; 170:578–589.
8. Liu X, Zhao Y, Gao J, Pawlyk B, Starcher B, Spencer JA, Yanagisawa H, Zuo J, Li T. Elastic fiber homeostasis requires lysyl oxidase-like 1 protein. Nat Genet 2004; 36:178–182.
9. Coates KW, Galan HL, Shull BL, Kuehl TJ. The squirrel monkey: an animal model of pelvic relaxation. Am J Obstet Gynecol 1995; 172:588–593.
10. Mattson JA, Kuehl TJ, Yandell PM, Pierce LM, Coates KW. Evaluation of the aged female baboon as a model of pelvic organ prolapse and pelvic reconstructive surgery. Am J Obstet Gynecol 2005; 192:1395–1398.
11. Wieslander CK, Marinis SI, Drewes PG, Keller PW, Acevedo JF, Word RA. Regulation of elastolytic proteases in the mouse vagina during pregnancy, parturition, and puerperium. Biol Reprod 2008; 78:521–528.
12. Norris ML, Adams CE. Exteroceptive factors, sexual maturation and reproduction in the female rat. Lab Anim 1979; 13:283–286.
13. Gutierrez J, Alvarez-Ordas I, Rojo M, Marin B, Menendez-Patterson A. Reproductive function and sexual behaviour in female rats exposed to immobilization stress or ACTH injections during gestation. Physiol Bohemoslov 1989; 38:13–20.
14. Hashizume K, Ohashi K. Timing of sexual receptivity and the release of gonadotrophins during puberty in female rats. J Reprod Fertil 1984; 72: 87–91.
15. Kitchlu S, Mehrotra PK. Easy criterion for detection of mating in guinea pig. Indian J Exp Biol 1991; 29:70–71.
16. Boreham MK, Wai CY, Miller RT, Schaffer JI, Word RA. Morphometric analysis of smooth muscle in the anterior vaginal wall of women with pelvic organ prolapse. Am J Obstet Gynecol 2002; 187:56–63.
17. Boreham MK, Miller RT, Schaffer JI, Word RA. Smooth muscle myosin heavy chain and caldesmon expression in the anterior vaginal wall of women with and without pelvic organ prolapse. Am J Obstet Gynecol 2001; 185:944–952.
18. Moalli PA, Talarico LC, Sung VW, Klingensmith WL, Shand SH, Meyn LA, Watkins SC. Impact of menopause on collagen subtypes in the arcus tendineous fasciae pelvis. Am J Obstet Gynecol 2004; 190:620–627.
19. Yanagisawa H, Davis EC, Starcher BC, Ouchi T, Yanagisawa M, Richardson JA, Olson EN. Fibulin-5 is an elastin-binding protein essential for elastic fibre development in vivo. Nature 2002; 415:168–171.
20. Chen B, Wen Y, Polan ML. Elastolytic activity in women with stress urinary incontinence and pelvic organ prolapse. Neurourol Urodyn 2004; 23:119–126.
21. Rahn DD, Acevedo JF, Word RA. Effect of vaginal distention on elastic fiber synthesis and matrix degradation in the vaginal wall: potential role in the pathogenesis of pelvic organ prolapse. Am J Physiol Regul Integr Comp Physiol 2008; 295:R1351–R1358.
22. Zong W, Zyczynski HM, Meyn LA, Gordy SC, Moalli PA. Regulation of MMP-1 by sex steroid hormones in fibroblasts derived from the female pelvic floor. Am J Obstet Gynecol 2007; 196:349.e1–349.e11.
23. Phillips CH, Anthony F, Benyon C, Monga AK. Collagen metabolism in the uterosacral ligaments and vaginal skin of women with uterine prolapse. BJOG 2006; 113:39–46.
24. Gabriel B, Watermann D, Hancke K, Gitsch G, Werner M, Tempfer C,

Hausen A. Increased expression of matrix metalloproteinase 2 in uterosacral ligaments is associated with pelvic organ prolapse. Int Urogynecol J Pelvic Floor Dysfunct 2006; 17:478–482.
25. Cox DA, Helvering LM. Extracellular matrix integrity: a possible mechanism for differential clinical effects among selective estrogen receptor modulators and estrogens? Mol Cell Endocrinol 2006; 247:53–59.
26. Moalli PA, Shand SH, Zyczynski HM, Gordy SC, Meyn LA. Remodeling of vaginal connective tissue in patients with prolapse. Obstet Gynecol 2005; 106:953–963.
27. Zhao YG, Xiao AZ, Cao XM, Zhu C. Expression of matrix metalloproteinase −2, −9 and tissue inhibitors of metalloproteinase −1, −2, −3 mRNAs in rat uterus during early pregnancy. Mol Reprod Dev 2002; 62: 149–158.
28. Rudolph-Owen LA, Hulboy DL, Wilson CL, Mudgett J, Matrisian LM. Coordinate expression of matrix metalloproteinase family members in the uterus of normal, matrilysin-deficient, and stromelysin-1-deficient mice. Endocrinology 1997; 138:4902–4911.
29. Fata JE, Ho AT, Leco KJ, Moorehead RA, Khokha R. Cellular turnover and extracellular matrix remodeling in female reproductive tissues: functions of metalloproteinases and their inhibitors. Cell Mol Life Sci 2000; 57:77–95.
30. Curry TE Jr, Osteen KG. Cyclic changes in the matrix metalloproteinase system in the ovary and uterus. Biol Reprod 2001; 64:1285–1296.
31. Curry TE Jr, Osteen KG. The matrix metalloproteinase system: changes, regulation, and impact throughout the ovarian and uterine reproductive cycle. Endocr Rev 2003; 24:428–465.
32. Houghton AM, Quintero PA, Perkins DL, Kobayashi DK, Kelley DG, Marconcini LA, Mecham RP, Senior RM, Shapiro SD. Elastin fragments drive disease progression in a murine model of emphysema. J Clin Invest 2006; 116:753–759.
33. Nenan S, Planquois JM, Berna P, De Mendez I, Hitier S, Shapiro SD, Boichot E, Lagente V, Bertrand CP. Analysis of the inflammatory response induced by rhMMP-12 catalytic domain instilled in mouse airways. Int Immunopharmacol 2005; 5:511–524.
34. Ntayi C, Labrousse AL, Debret R, Birembaut P, Bellon G, Antonicelli F, Hornebeck W, Bernard P. Elastin-derived peptides upregulate matrix metalloproteinase-2-mediated melanoma cell invasion through elastin-binding protein. J Invest Dermatol 2004; 122:256–265.
35. Vu TH, Werb Z. Gelatinase B: Structure, Regulation, and Function. San Diego: Academic Press; 1998.
36. Vu TH, Shipley JM, Bergers G, Berger JE, Helms JA, Hanahan D, Shapiro SD, Senior RM, Werb Z. MMP-9/gelatinase B is a key regulator of growth plate angiogenesis and apoptosis of hypertrophic chondrocytes. Cell 1998; 93:411–422.
37. Itoh T, Ikeda T, Gomi H, Nakao S, Suzuki T, Itohara S. Unaltered secretion of beta-amyloid precursor protein in gelatinase A (matrix metalloproteinase 2)-deficient mice. J Biol Chem 1997; 272:22389–22392.
38. Allaire E, Hasenstab D, Kenagy RD, Starcher B, Clowes MM, Clowes AW. Prevention of aneurysm development and rupture by local overexpression of plasminogen activator inhibitor-1 [see comment]. Circulation 1998; 98:249–255.
39. Guo G, Booms P, Halushka M, Dietz HC, Ney A, Stricker S, Hecht J, Mundlos S, Robinson PN. Induction of macrophage chemotaxis by aortic extracts of the mgR Marfan mouse model and a GxxPG-containing fibrillin-1 fragment. Circulation 2006; 114:1855–1862.